

# Correlation between Fermi surface transformations and superconductivity in the electron-doped high- $T_c$ superconductor $\text{Nd}_{2-x}\text{Ce}_x\text{CuO}_4$

T. Helm,<sup>1,\*</sup> M. V. Kartsovnik,<sup>1,†</sup> C. Proust,<sup>2</sup> B. Vignolle,<sup>2</sup> C. Putzke,<sup>3,‡</sup> E. Kampert,<sup>3</sup> I. Sheikin,<sup>4</sup> E.-S. Choi,<sup>5</sup> J. S. Brooks,<sup>5</sup> N. Bittner,<sup>1,§</sup> W. Biberacher,<sup>1</sup> A. Erb,<sup>1,6</sup> J. Wosnitza,<sup>3</sup> and R. Gross<sup>1,6,¶</sup>

<sup>1</sup> *Walther-Meißner-Institut, Bayerische Akademie der Wissenschaften, D-85748 Garching, Germany*

<sup>2</sup> *Laboratoire National des Champs Magnétiques Intenses, CNRS, INSA, UJF, UPS, F-31400 Toulouse, France*

<sup>3</sup> *Hochfeld-Magnetlabor Dresden, Helmholtz-Zentrum Dresden-Rossendorf, D-01328 Dresden, Germany*

<sup>4</sup> *Laboratoire National des Champs Magnétiques Intenses, CNRS, INSA, UJF, UPS, F-38042 Grenoble Cedex 9, France*

<sup>5</sup> *National High Magnetic Field Laboratory and Department of Physics, Florida State University, Tallahassee, Florida 32310, USA*

<sup>6</sup> *Physik-Department, Technische Universität München, D-85748 Garching, Germany*

(Dated: March 31, 2014)

Two critical points have been revealed in the normal-state phase diagram of the electron-doped cuprate superconductor  $\text{Nd}_{2-x}\text{Ce}_x\text{CuO}_4$  by exploring the Fermi surface properties of high quality single crystals by high-field magnetotransport. First, the quantitative analysis of the Shubnikov-de Haas effect shows that the weak superlattice potential responsible for the Fermi surface reconstruction in the overdoped regime extrapolates to zero at the doping level  $x_c = 0.175$  corresponding to the onset of superconductivity. Second, the high-field Hall coefficient exhibits a sharp drop right below optimal doping  $x_{\text{opt}} = 0.145$  where the superconducting transition temperature is maximum. This drop is most likely associated with the onset of long-range antiferromagnetic ordering. Thus, for  $\text{Nd}_{2-x}\text{Ce}_x\text{CuO}_4$  the superconducting dome appears to be pinned by two critical points to the normal state phase diagram.

PACS numbers: 74.72.Ek, 71.18.+y, 72.15.Gd

In order to clarify the mechanism responsible for high-temperature superconductivity in the superconducting (SC) cuprates profound knowledge on the exact nature of the underlying “normal”, i.e., non-superconducting state is mandatory. This long-standing issue, however, remains controversial. Even for the relatively simple case of the electron-doped cuprates  $\text{Ln}_{2-x}\text{Ce}_x\text{CuO}_4$  ( $\text{Ln} = \text{Nd}, \text{Pr}, \text{Sm}, \text{La}$ ), where the SC state emerges in direct neighbourhood of a state with commensurate antiferromagnetic (AF) order, it is not clear whether the two states coexist and, if yes, to which extent [1]. A number of neutron scattering studies have been reported, providing arguments both for [2–5] and against [6] the coexistence. Angle-resolved photoemission spectroscopy (ARPES) data [7–9] show a reconstruction of the quasi-two-dimensional Fermi surface consistent with a commensurate AF ordering up to the optimal doping level  $x_{\text{opt}}$  corresponding to the maximum SC transition temperature. Magnetotransport studies go even further, indicating the presence of two types of charge carriers [10–16] and, hence, a reconstructed Fermi surface even in the overdoped region of the phase diagram, where ARPES [8] finds the unreconstructed hole Fermi surface, even though with a somewhat reduced spectral weight around the nodal points.

For cuprate superconductors sample quality or surface effects are often invoked to explain apparently contradictory results. However, recently clear evidence for a reconstructed Fermi surface in the overdoped regime of the prototypical electron-doped cuprate  $\text{Nd}_{2-x}\text{Ce}_x\text{CuO}_4$

(NCCO) was obtained from the observation of slow Shubnikov-de Haas (SdH) oscillations in high-quality single crystals [17]. The Fermi surface area derived from the oscillation frequency is only about 1% of the first Brillouin zone, which is inconsistent with the large unreconstructed Fermi surface seen in ARPES experiments for the same doping level [8, 18]. These oscillations have been ascribed to small hole pockets formed around the points  $(\pm\pi/2a, \pm\pi/2a)$  of the Brillouin zone after the reconstruction of the original Fermi surface by a commensurate superlattice potential  $V_{\mathbf{Q}}$  with the wave vector  $\mathbf{Q} = (\pi/a, \pi/a)$  [17]. For strongly overdoped but still SC samples,  $x = 0.17$ , high-frequency oscillations fully consistent with the large-area unreconstructed Fermi surface were observed in the initial SdH experiments [17]. This change in the SdH oscillation spectrum in the doping interval between 0.16 and 0.17 was apparently in agreement with Hall effect [10] and thermopower [15] data, suggesting a quantum critical point hidden under the SC dome in the overdoped region of the phase diagram. However, later on more elaborate SdH experiments [19, 20] have further extended the range in which the Fermi surface stays reconstructed up to at least  $x = 0.17$ , the highest doping level attainable for bulk NCCO crystals.

Here, we report systematic high-field magnetotransport studies on high-quality NCCO crystals, which allow us to precisely locate two critical doping levels in the normal-state phase diagram of this material and correlate them with the position of the SC dome. First, by

performing a quantitative analysis of SdH oscillations observed in the magnetic-breakdown (MB) regime of overdoped samples, we evaluate the small MB gap  $\Delta_{\text{MB}} \simeq V_{\text{Q}}$  between different parts of the reconstructed Fermi surface as a function of  $x$ . The  $x$ -dependence of the gap is found to mimic that of the SC critical temperature  $T_c(x)$ , both extrapolating to zero at the same characteristic doping level  $x_c \approx 0.175$ . Second, we present high-field Hall resistance measurements which, in combination with the SdH data, reveal a large energy gap emerging in the system right below the optimal doping level  $x_{\text{opt}} = 0.145$ .

The NCCO crystals with Ce concentrations covering the whole SC range of doping,  $0.13 \leq x \leq 0.17$ , were grown using the travelling solvent floating zone technique, annealed, and characterized as described in Ref. 21. For each  $x$ , several samples showing the best high- to low-temperature resistance ratio and narrow SC transitions were selected. The sample geometry was chosen according to the type of experiment, see Supplemental Material [22] for details. All the experiments were done in magnetic fields perpendicular to the  $\text{CuO}_2$  layers. Most of the results presented here were obtained in pulsed magnetic fields. Additionally, measurements in steady fields at precisely controlled temperatures were done for evaluating effective cyclotron masses.

Figure 1 shows examples of SdH oscillations in the interlayer resistance of optimally doped and overdoped NCCO at  $T \simeq 2.5$  K. For  $x \geq 0.15$ , the oscillations contain two characteristic frequencies:  $F_\alpha \simeq 250 - 300$  T and  $F_\beta \simeq 11$  kT. The slow  $\alpha$  oscillations are associated with small orbits on the reconstructed Fermi surface [17]. The fast  $\beta$  oscillations reveal a cyclotron orbit, which is geometrically equivalent to that on the large unreconstructed Fermi surface and arises from the MB effect [19, 20, 23]. The fast oscillations are dominant at high fields for  $x = 0.17$  and rapidly diminish at decreasing doping. For  $x = 0.15$ , they are about 100-times weaker than the slow oscillations at the same field strength. For optimal doping,  $x_{\text{opt}} = 0.145$ , they are no longer resolvable above the noise level,  $\lesssim 10^{-4}$  of the total resistance signal.

On the qualitative level the observed behavior is easily understood as a result of an enhancement of the superlattice potential  $V_{\text{Q}}$ , hence, of the MB gap with decreasing  $x$ . Moreover, due to the very good signal-to-noise ratio of our measurements, the data can be analyzed quantitatively, allowing us to estimate the MB gap as a function of  $x$ . First, the analysis of the  $T$ -dependence of the oscillation amplitudes in terms of the Lifshitz-Kosevich formula [24] provides the relevant effective cyclotron masses  $m_\alpha$  and  $m_\beta$ . Further, the frequencies and phase factors are determined directly from the positions of the minima and maxima of the oscillating resistance. Finally, the relative amplitudes of the  $\alpha$  and  $\beta$  oscillations measured at a constant temperature as a function of magnetic field are fitted, taking into account the temperature and Din-

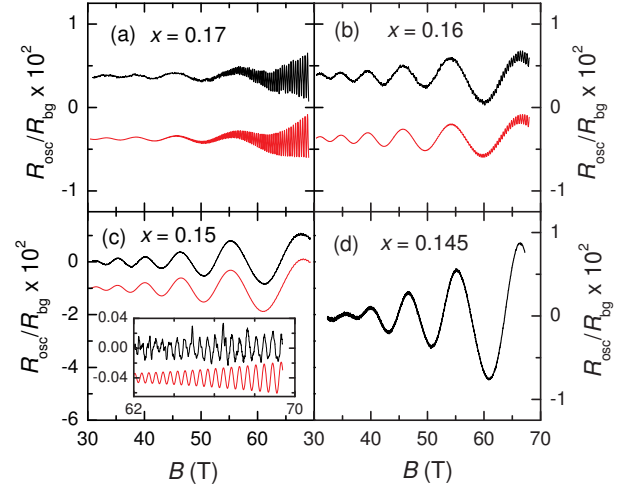


FIG. 1. (Color online) Black lines: SdH oscillations of the interlayer resistance of NCCO crystals with different doping levels  $x$  at  $T \approx 2.5$  K. The data are normalized to the non-oscillating field-dependent background resistance  $R_{\text{bg}}$ . Red lines: fits to the experimental data according to the Lifshitz-Kosevich theory extended to the MB regime. The curves are vertically shifted for clarity. Inset: enlarged view of the fast MB oscillations for  $x = 0.15$  after subtracting the slowly oscillating component.

gle damping factors as well as the MB effect [24]. The fitting procedure is described in detail in Supplemental Material [22]. The results for  $x = 0.17$ ,  $0.16$ , and  $0.15$  are presented by the red curves in Fig. 1(a)-(c). Clearly, the fits nicely reproduce the relative amplitudes as well as the field dependence of both oscillating components.

The values of the MB field  $B_0$  obtained from the fitting are shown in Fig. 2(a) by squares. From this data the energy gap  $\Delta_{\text{MB}}$  between different parts of the reconstructed Fermi surface can be estimated according to Blount's criterion  $\Delta_{\text{MB}} \approx (\hbar e B_0 \varepsilon_F / m_\beta)^{1/2}$  [24]. Here,  $e$  is the elementary charge and  $\varepsilon_F \approx 0.5$  eV the Fermi energy. The  $\Delta_{\text{MB}}$  values (blue triangles) are plotted in Fig. 2(a) as a function of  $x$  along with the SC critical temperature  $T_c(x)$  (black circles, right-hand scale). We see that the MB gap is small (meV range) and decreases approximately linearly with increasing  $x$  in the overdoped regime. Most importantly,  $\Delta_{\text{MB}}(x)$  extrapolates to zero at the same characteristic doping level  $x_c = 0.175$ , at which  $T_c$  is believed to vanish [21, 25].

Figure 2(b) shows the doping dependence of the amplitude  $A_\alpha$  of the  $\alpha$  oscillations normalized to the non-oscillating resistance background together with the corresponding effective cyclotron mass  $m_\alpha$ . Obviously,  $m_\alpha$  increases rapidly on moving from the strongly overdoped regime towards optimal doping. This change cannot simply be explained by the experimentally observed weak  $x$ -dependence of the area of the  $\alpha$  orbit [20]. It is most likely a mass renormalization effect due to enhanced electron correlations in the vicinity of a metal-insulator transition.

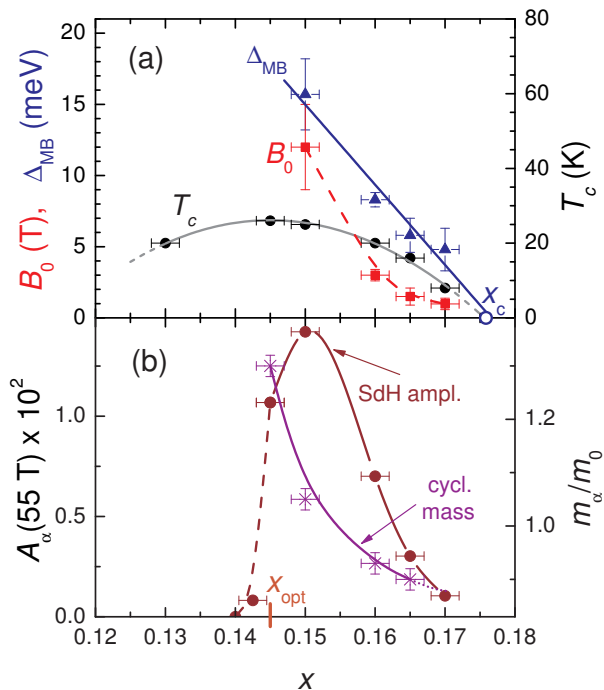


FIG. 2. (Color online) (a) MB field  $B_0$  (squares), the corresponding energy gap  $\Delta_{MB}$  (triangles), and the SC critical temperature  $T_c$  plotted as a function of Ce concentration  $x$ . The straight line is a linear fit to the  $\Delta_{MB}(x)$  dependence, extrapolating to zero at  $x_c \approx 0.175$ . The other lines are guides to the eye. (b)  $x$ -dependence of the amplitude  $A_\alpha$  of the slow oscillations measured at  $B = 55$  T,  $T = 2.5$  K (circles) and the relevant cyclotron mass  $m_\alpha$  normalized to the free electron mass  $m_0$  (stars). The lines are guides to the eye.

In fact, it resembles the behavior observed recently on a hole-doped cuprate [26] and an iron-pnictide [27] high- $T_c$  superconductors near a quantum critical point.

The  $x$ -dependence of  $A_\alpha$  in the overdoped regime is governed by that of the MB gap: it rapidly grows upon going from  $x = 0.17$  to 0.15. At optimal doping it is slightly smaller than at  $x = 0.15$ , which is consistent with the considerable,  $\sim 20\%$ , increase of the cyclotron mass and consequent reduction of the temperature and Dingle damping factors. A further decrease of  $x$  leads to a dramatic suppression of  $A_\alpha$ . When the doping level is decreased by just  $\Delta x \approx 0.3\%$  below  $x_{opt}$ , the amplitude drops by more than an order of magnitude, becoming too small for a quantitative analysis. At present, it cannot even be ruled out that the weak oscillations remaining below  $x_{opt}$  are caused by a minor optimally doped sample fraction due to an unavoidable small inhomogeneity of the Ce distribution. Assuming for a moment that the oscillations are, however, inherent to a perfectly homogeneous  $x = 0.142$  sample, we estimate that the cyclotron mass should increase by almost a factor of 2 as compared to that at  $x = 0.145$ , in order to account for the observed reduction of the amplitude. Such a steep rise would be

a strong argument in favor of the mass divergence near the optimal doping level.

Of course, a diverging effective mass is only one of possible explanations of the observed suppression of the oscillations. An alternative mechanism may involve an abrupt change in the electronic spectrum or in scattering processes. We note that a trivial scenario associated with a poor crystal quality is highly unlikely in our case. From the crystal growth point of view [16, 28], the sample quality should not vary considerably with  $x$  around  $x_{opt}$ . A reduction of crystal quality is expected only for strongly overdoped samples approaching the solubility limit  $x \approx 0.18$ . Consistently, the Dingle temperatures, sensitive to crystal imperfections [24], obtained from our fits in Fig. 1 are close to each other,  $T_D = 13 \pm 1$  K, for crystals with  $x = 0.145$  to 0.16 and rise to 17-18 K for  $x = 0.165$  and 0.17 [22]. This suggests that also for slightly underdoped samples,  $0.14 \leq x < 0.145$ , quality is unlikely a critical issue and the reason for the suppression of the quantum oscillations must lie in an intrinsic significant change in the electronic system.

To gain further insight in this change, we have studied the high-field Hall effect in NCCO crystals with different Ce concentrations, focusing on the regime around  $x_{opt}$ . Figure 3 shows examples of the field-dependent Hall resistivity  $\rho_{xy}(B)$  measured at  $T \approx 2$  K. At this low temperature various complications associated with inelastic scattering and thermal fluctuations [29] can be neglected. Outside the very narrow range around  $x_{opt}$ , our data is in good agreement with previous studies on NCCO single crystals [31] and on thin films of the sister compound  $\text{Pr}_{2-x}\text{Ce}_x\text{CuO}_4$  [10, 14, 30]. Note that the small positive Hall resistivity measured for the overdoped ( $x = 0.165$ ) sample indicating a single large holelike orbit, is fully consistent with a multiply-connected reconstructed Fermi surface, taking into account the very low MB field  $B_0 \approx 1.5$  T determined for this doping. Near optimal doping ( $x = 0.15$ ) the MB field exceeds 10 T. At  $B < B_0$  the normal-state Hall conductivity is determined by competing contributions from electron- and hole-like orbits on the reconstructed Fermi surface, resulting in a small negative  $\rho_{xy}(B)$ . This is in agreement with calculations based on a two-band model [11]. At  $B > B_0$ ,  $\rho_{xy}(B)$  turns up, crosses zero, and eventually assumes a linear positive slope in the strong MB regime, where again the large holelike orbit dominates. This field dependence correlates with the nonmonotonic magnetoresistance observed at this doping [14, 17]. A very similar behavior is found for  $x = x_{opt}$ . A comparison of the two curves shown in the inset of Fig. 3 suggests that at optimal doping the MB field is  $\sim 5$  T higher than at  $x = 0.15$ .

The most remarkable feature of the Hall effect data is the fact that  $\rho_{xy}(B)$  changes dramatically on reducing the doping level below  $x_{opt}$ . Already for  $x = 0.142$ , the weak positive signal observed for  $x \geq x_{opt}$  at high fields is replaced by a large negative signal with no sign of satu-

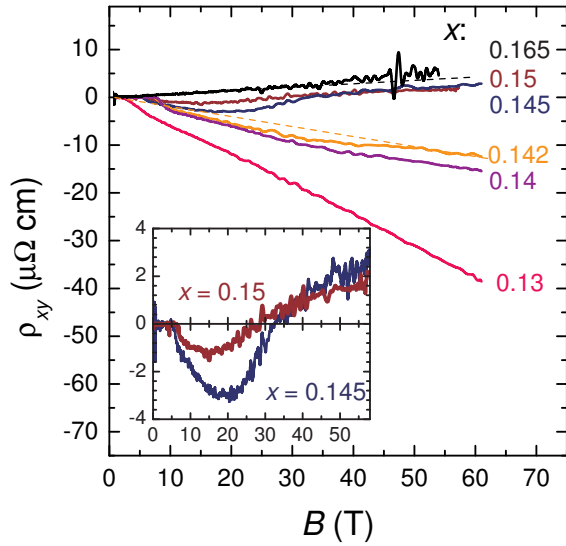


FIG. 3. (Color online) Field-dependent Hall resistivity at  $T = 2$  K, for different  $x$ . Inset: enlarged view on the data for  $x = 0.145$  and  $0.15$ .

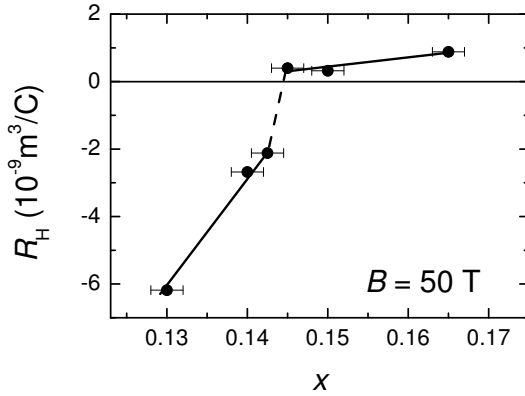


FIG. 4. Hall coefficient measured at  $B = 50$  T and  $T = 2$  K as a function of  $x$ . Lines are guides to the eye.

ration at the highest fields [32]. This change is especially manifest in the  $x$ -dependence of the high-field Hall coefficient,  $R_H = \rho_{xy}/B$ , plotted in Fig. 4. The sharp step observed between  $x = 0.145$  and  $0.142$  is a result of a steplike increase of the MB field  $B_0$  beyond the accessible field range. Thus, our data indicate a sudden increase of the gap between the electron and hole pockets of the reconstructed Fermi surface.

It is natural to associate the opening of a large gap right below  $x_{\text{opt}}$  with a static AF order coexisting with superconductivity as proposed by several authors [2, 3, 33]. This conclusion is apparently in line with the ARPES data [7–9], implying a Fermi surface reconstruction due to an AF superlattice potential persisting up to  $x_{\text{opt}}$ . It was argued that a spurious magnetic superstructure signal in SC NCCO might come from minor epitaxial precipitations of paramagnetic  $(\text{Nd,Ce})_2\text{O}_3$  unavoidably

present in oxygen-reduced crystals [34] or from remnants of an insufficiently reduced phase [6]. However, our transport data, insensitive to insulating or poorly conducting precipitations, unambiguously reveal the gap as an inherent feature of the major conducting phase, setting in right below optimal doping.

Going back to the overdoped regime, the  $x$ -dependence of the small MB gap [see Fig. 2(a)] is suggestive of a translational-symmetry-breaking quantum phase transition at the doping level  $x_c$ , corresponding to the onset of superconductivity in the overdoped regime. The same position of the quantum critical point was recently inferred from the  $T$ -linear resistivity of electron-doped  $\text{Ln}_{2-x}\text{Ce}_x\text{CuO}_4$  ( $\text{Ln} = \text{La}, \text{Pr}$ ) thin films [35]. It should be noted, however, that the nature of the relevant order parameter is unclear. While, as argued above, the long-range antiferromagnetism is most likely established right below optimal doping, no convincing evidence for it has been found at  $x_{\text{opt}} < x < x_c$  [1]. Possible alternatives can be a hidden  $d$ -density-wave order [36] or charge modulation as found recently in hole-underdoped cuprates [37, 38]. On the other hand, the observation of the slow SdH oscillations (and thereby a finite MB gap) may be consistent with a fluctuating AF order reported by several groups [1, 3, 6], provided the corresponding time scale and correlation length are sufficiently large. An estimate for the lower limit of the time over which a charge carrier “sees” the potential  $V_{\mathbf{Q}}$  with the wave vector  $\mathbf{Q}$  is obtained from the Dingle temperature. Taking the value  $T_D = 18$  K determined for the strongly overdoped,  $x = 0.17$ , sample, we obtain  $\tau_D = \hbar/2\pi k_B T_D \approx 0.7 \times 10^{-13}$  s. The corresponding lower limit for the correlation length,  $\xi_{\text{min}} \sim \tau_D v_F \simeq 15$  nm, is about 40 times the unit cell period.

In conclusion, our comprehensive high-field magneto-transport study reveals the existence of two critical points in the normal-state phase diagram of NCCO. The doping values of these points remarkably correlate with those characterizing the SC dome. On reducing  $x$ , superconductivity emerges at the same critical doping level,  $x_c \approx 0.175$ , as the weak superlattice potential  $V_{\mathbf{Q}} \sim \Delta_{\text{MB}}$ . Below  $x_c$ , the SC critical temperature  $T_c$  grows together with this potential. While the exact origin of  $V_{\mathbf{Q}}$  is still to be determined, it obviously must have a strong impact on the SC pairing. The maximum in the  $T_c(x)$  dependence at  $x_{\text{opt}} = 0.145$  coincides with the second critical point where a large energy gap sets in. This can naturally be explained by an intrinsic competition between superconductivity and long-range antiferromagnetism. As argued above, the large energy gap is an inherent feature of the major conducting phase. A highly interesting question is related to the possible microscopic coexistence of antiferromagnetism and superconductivity in high-quality NCCO crystals. Further studies are required to settle this issue.

This work was supported by the German Research

Foundation via grant GR 1132/15. We acknowledge support of our high-field experiments by HLD-HZDR (Dresden) and LNCMI-CNRS (Toulouse, Grenoble), members of the European Magnetic Field Laboratory. Part of experiments was performed at the NHMFL (Tallahassee), under the support by nsf-dmr 1005293, NSF Cooperative Agreement No. DMR-0654118, the State of Florida, and the U.S. Department of Energy.

---

\* Present address: Material Science Division, Lawrence Berkeley National Laboratory 62R0203, 94720 Berkeley, CA, USA

† Mark.Kartsovnik@wmi.badw-muenchen.de

‡ Present address: University of Bristol, Bristol, BS8 1TL, UK

§ Present address: Max-Planck-Institut für Festkörperforschung, D-70569 Stuttgart, Germany

¶ Rudolf.Gross@wmi.badw-muenchen.de

- [1] N. P. Armitage, P. Fournier, and R. L. Greene, *Rev. Mod. Phys.* **82**, 2421 (2010).
- [2] T. Uefuji, K. Kurahashi, M. Fujita, M. Matsuda, and K. Yamada, *Physica C* **378381**, 273 (2002).
- [3] M. Fujita, M. Matsuda, S.-H. Lee, M. Nakagawa, and K. Yamada, *Phys. Rev. Lett.* **101**, 107003 (2008).
- [4] M. Fujita, M. Matsuda, S. Katano, and K. Yamada, *Phys. Rev. Lett.* **93**, 147003 (2004).
- [5] H. J. Kang, P. Dai, H. A. Mook, D. N. Argyriou, V. Sikolenko, J. W. Lynn, Y. Kurita, S. Komiya, and Y. Ando, *Phys. Rev. B* **71**, 214512 (2005).
- [6] E. M. Motoyama, G. Yu, I. M. Vishik, O. P. Vajk, P. K. Mang, and M. Greven, *Nature* **445**, 186 (2007).
- [7] P. N. Armitage, F. Ronning, D. H. Lu, C. Kim, A. Damascelli, K. M. Shen, D. L. Feng, H. Eisaki, Z.-X. Shen, P. K. Mang, et al., *Phys. Rev. Lett.* **88**, 257001 (2002).
- [8] H. Matsui, T. Takahashi, T. Sato, K. Terashima, H. Ding, T. Uefuji, and K. Yamada, *Phys. Rev. B* **75**, 224514 (2007).
- [9] A. F. Santander-Syro, M. Ikeda, T. Yoshida, A. Fujimori, K. Ishizaka, M. Okawa, S. Shin, R. L. Greene, and N. Bontemps, *Phys. Rev. Lett.* **106**, 197002 (2011).
- [10] Y. Dagan, M. M. Qazilbash, C. P. Hill, V. N. Kulkarni, and R. L. Greene, *Phys. Rev. Lett.* **92**, 167001 (2004).
- [11] J. Lin and A. J. Millis, *Phys. Rev. B* **72**, 214506 (2005).
- [12] H. Balci, C. P. Hill, M. M. Qazilbash, and R. L. Greene, *Phys. Rev. B* **68**, 054520 (2003).
- [13] P. Li and R. L. Greene, *Phys. Rev. B* **76**, 174512 (2007).
- [14] P. Li, F. F. Balakirev, and R. L. Greene, *Phys. Rev. Lett.* **99**, 047003 (2007).
- [15] P. Li, K. Behnia, and R. L. Greene, *Phys. Rev. B* **75**, 020506(R) (2007).
- [16] M. Lambacher, PhD Thesis, Technische Universität München (2008).
- [17] T. Helm, M. V. Kartsovnik, M. Bartkowiak, N. Bittner, M. Lambacher, A. Erb, J. Wosnitza, and R. Gross, *Phys. Rev. Lett.* **103**, 157002 (2009).
- [18] S. Massidda, N. Hamada, J. Yu, and A. J. Freeman, *Physica C* **157**, 571 (1989).
- [19] T. Helm, M. V. Kartsovnik, I. Sheikin, M. Bartkowiak, F. Wolff-Fabris, N. Bittner, W. Biberacher, M. Lambacher, A. Erb, J. Wosnitza, et al., *Phys. Rev. Lett.* **105**, 247002 (2010).
- [20] M. V. Kartsovnik, T. Helm, C. Putzke, F. W.-F. I. Sheikin, S. Lepault, C. Proust, D. Vignolles, N. Bittner, W. Biberacher, A. Erb, et al., *New J. Phys.* **13**, 015001 (2011).
- [21] M. Lambacher, T. Helm, M. Kartsovnik, and A. Erb, *Eur. Phys. J. Special Topics* **188**, 61 (2010).
- [22] See Supplemental Material at [URL will be inserted by publisher].
- [23] J. Eun and S. Chakravarty, *Phys. Rev. B* **84**, 094506 (2011).
- [24] D. Shoenberg, *Magnetic Oscillations in Metals* (Cambridge University Press, Cambridge, 1984).
- [25] H. Takagi, S. Uchida, and Y. Tokura, *Phys. Rev. Lett.* **62**, 1197 (1989).
- [26] S. E. Sebastian, N. Harrison, M. M. Altarawneh, C. H. Mielke, R. Liang, D. A. Bonn, W. N. Hardy, and G. G. Lonzarich, *Phys. Rev. B* **107**, 6175 (2010).
- [27] P. Walmsley, C. Putzke, L. Malone, I. Guillaumon, D. Vignolles, C. Proust, S. Badoux, A. I. Coldea, M. D. Watson, S. Kasahara, et al., *Phys. Rev. Lett.* **110**, 257002 (2013).
- [28] A. Erb, in *Handbook of Applied Superconductivity* (Wiley-VCH, Weinheim, 2014), in press.
- [29] H. Kontani, *Rep. Prog. Phys.* **71**, 026501 (2008); G. S. Jenkins, D. C. Schmadel, P. L. Bach, R. L. Greene, X. Bächamp-Laganière, G. Roberge, P. Fournier, H. Kontani, and H. D. Drew, *Phys. Rev. B* **81**, 024508 (2010);
- [30] S. Charpentier, G. Roberge, S. Godin-Proulx, X. Béchamp-Laganière, K. D. Truong, P. Fournier, and P. Rauwel, *Phys. Rev. B* **81**, 104509 (2010).
- [31] C. H. Wang, G. Y. Wang, T. Wu, Z. Feng, X. G. Luo, and X. H. Chen, *Phys. Rev. B* **72**, 132506 (2005).
- [32] A weak curvature of  $\rho_{xy}(B)$  at fields between 20 and 50 T can be attributed to an unavoidable finite (typically  $\leq 0.3\%$ ) distribution width of Ce concentration through the sample volume. Note that at fields  $> 50$  T the signal acquires a linear slope extrapolating to zero, cf. straight dashed line in Fig. 3.
- [33] A. Zimmers, J. M. Tomczak, R. P. S. M. Lobo, N. Bontemps, C. P. Hill, M. C. Barr, Y. Dagan, R. L. Greene, A. J. Millis, and C. C. Homes, *Europhys. Lett.* **70**, 225231 (2005).
- [34] P. K. Mang, S. Larochelle, A. Mehta, O. P. Vajk, A. S. Erickson, L. Lu, W. J. L. Buyers, A. F. Marshall, K. Prokes, and M. Greven, *Phys. Rev. B* **70**, 094507 (2004).
- [35] K. Jin, N. P. Butch, K. Kirshenbaum, J. Paglione, and R. L. Greene, *Nature* **476**, 73 (2011); N. P. Butch, K. Jin, K. Kirshenbaum, R. L. Greene, and J. Paglione, *PNAS* **109**, 8440 (2012).
- [36] S. Chakravarty, R. B. Laughlin, D. K. Morr, and C. Nayak, *Phys. Rev. B* **63**, 094503 (2001).
- [37] T. Wu, H. Mayaffre, S. Krämer, M. Horvatić, C. Berthier, W. N. Hardy, R. Liang, D. A. Bonn, and M.-H. Julien, *Nature* **477**, 191 (2011).
- [38] G. Ghiringhelli, M. L. Tacon, M. Minola, S. Blanco-Canosa, C. Mazzoli, N. B. Brookes, G. M. D. Luca, A. Frano, D. G. Hawthorn, F. He, et al., *Science* **337**, 821 (2012); J. Chang, E. Blackburn, A. T. Holmes, N. B. Christensen, J. Larsen, J. Mesot, R. Liang, D. A. Bonn, W. N. Hardy, A. Watenphul, et al., *Nat. Phys.* **8**, 871 (2012).